

Invariant computation of differential characteristics in 3D images.

L. Alvarez, K. Krissian and A. Trujillo.

Departamento de Informática y Sistemas
Universidad de Las Palmas de Gran Canaria
Campus de Tafira, 35017 Las Palmas
Email: {lalvarez-kkrissian-atrujillo}@dis.ulpgc.es
WWW: <http://serdis.dis.ulpgc.es/ami>

February 2001

Abstract

Differential characteristics like gradients, principal curvatures and principal directions of the iso-intensity surfaces are very useful informations in many 3D computer vision tasks. In this paper we propose a new technique to compute the first and second derivatives of a 3D function based on the orientation invariance of such differential characteristics. We use a model of 'ideal' 3D edge in order to compute the derivative estimations. We present some numerical experiments on synthetic and real images in order to show the performance of the method.

1 Introduction

Differential characteristics like gradients, principal curvatures and principal directions of the iso-intensity surfaces are very useful informations in many 3D computer vision tasks. A very important property of this differential characteristics is that they are invariant under rotation transformations. For instance, the norm of the gradient does not depend on the orientation of the 3D image. On the other hand a lot of algorithms are very sensitive to the gradient magnitude because they use the norm of the gradient in order to discriminate between points in the image. However, most of the derivative estimations proposed in the literature do not take into account this important property of invariance under rotation, and are sensitive to the image orientation.

Principal curvatures and principal directions of isointensity surfaces are also very important features in 3D image applications, in particular in 3D medical imaging (see [2] and [4]). Principal curvatures and principal directions of an isointensity surface $F(x_1, x_2, x_3) = C$ can be directly computed from the first and second derivatives of function $F(\cdot)$, without any explicit parametrization of the surface. This kind of estimations have been successfully used in [5],[6] and [7] to compute differential characteristics of the isosurface. As in the case of the gradient norm, the values of the principal curvatures are independent of the particular orientation of the surface. In this paper we propose a new technique to compute the first and second derivatives of a 3D function based on the orientation invariance of the gradient and the principal curvatures.

In order to compute the derivatives, we will use a $3 \times 3 \times 3$ neighborhood of the voxel. To study the orientation invariance of the differential characteristic, we will use a model of an 'ideal' 3D edge. This model is defined by the family of functions

$$F^{\mathbf{e}}(\mathbf{x}) = \begin{cases} 1 & \text{if } (e_1x_1 + e_2x_2 + e_3x_3) \leq 0 \\ 0 & \text{if } (e_1x_1 + e_2x_2 + e_3x_3) > 0 \end{cases}$$

the 'ideal' edge associated with this function is given by a plane passing by $\mathbf{x} = \mathbf{0}$, $\mathbf{e} = (e_1, e_2, e_3)$ represents the normal direction to this plane. We study the invariance of the differential characteristic on this family of functions based on the value of \mathbf{e} , of course, we can not expect to get an exact invariance for any value of \mathbf{e} . We will study the case of $e_i \in \{-1, 0, 1\}$ which corresponds to the case where the edge plane fits the voxel lattice properly.

The organization of the paper is as follows: In section 2 we study the 3D invariant computation of the gradient, in section 3 we study the 3D invariant computation of the principal curvatures and directions. In section 4 we present some numerical results and finally, in section 5, we present some conclusions.

2 3-D invariant computation of the gradient.

Let $\mathbf{x} = (x_1, x_2, x_3)$ be a 3D point, and $F(\mathbf{x})$ be a 3D function. A good estimation of $\nabla F(\mathbf{x})$ is very important in a lot of 3D computer vision applications. In particular, a lot of algorithms depend on the magnitude of the gradient in order to discriminate points in the image. A very interesting property that should be satisfied by the gradient estimation is that the magnitude of the gradient does not depend on the orientation of the object in the image. In this section, we show the way to obtain a gradient estimation, which is invariant under rotation (or at least as invariant as possible).

In order to get our invariant numerical gradient estimation, we impose that the magnitude of the gradient of the 'ideal' edge $F^{\mathbf{e}}(\mathbf{x})$ in $\mathbf{x} = \mathbf{0}$ be independent of the orientation

vector \mathbf{e} . Of course, it is not possible to have such an invariance for any value of \mathbf{e} , we limit our study to the cases of $e_i \in \{-1, 0, 1\}$ with $\mathbf{e} \neq \mathbf{0}$. In order to obtain the gradient discretization we use a mask based on a $3 \times 3 \times 3$ neighborhood of a voxel. To simplify the discussion we consider that the size of the discretization of the spatial variables h is equal in all directions. We use the notation $F_{i,j,k} = F(ih, jh, kh)$. If we impose that the magnitude of the gradient estimation of $F^{\mathbf{e}}(\mathbf{x})$ in $\mathbf{x} = \mathbf{0}$ be independent of the orientation vector \mathbf{e} for $e_i \in \{-1, 0, 1\}$, a straightforward computation yields to the following gradient estimation.

$$\begin{aligned} \frac{\partial F}{\partial x}(ih, jh, kh) &= (1 - \alpha - \beta) \frac{F_{i+1,j,k} - F_{i-1,j,k}}{2h} + \\ &\frac{\alpha}{4} \left(\frac{F_{i+1,j,k+1} - F_{i-1,j,k+1} + F_{i+1,j,k-1} - F_{i-1,j,k-1}}{2h} \right) + \\ &\frac{\alpha}{4} \left(\frac{F_{i+1,j+1,k} - F_{i-1,j+1,k} + F_{i+1,j-1,k} - F_{i-1,j-1,k}}{2h} \right) + \\ &\frac{\beta}{4} \left(\frac{F_{i+1,j+1,k+1} - F_{i-1,j+1,k+1} + F_{i+1,j-1,k+1} - F_{i-1,j-1,k+1}}{2h} \right) \\ &\frac{\beta}{4} \left(\frac{F_{i+1,j+1,k-1} - F_{i-1,j+1,k-1} + F_{i+1,j-1,k-1} - F_{i-1,j-1,k-1}}{2h} \right) \end{aligned}$$

$$\begin{aligned} \frac{\partial F}{\partial y}(hi, hj, hk) &= (1 - \alpha - \beta) \frac{F_{i,j+1,k} - F_{i,j-1,k}}{2h} + \\ &\frac{\alpha}{4} \left(\frac{F_{i,j+1,k+1} - F_{i,j-1,k+1} + F_{i,j+1,k-1} - F_{i,j-1,k-1}}{2h} \right) + \\ &\frac{\alpha}{4} \left(\frac{F_{i+1,j+1,k} - F_{i-1,j+1,k} + F_{i+1,j-1,k} - F_{i-1,j-1,k}}{2h} \right) + \\ &\frac{\beta}{4} \left(\frac{F_{i+1,j+1,k+1} - F_{i-1,j+1,k+1} + F_{i+1,j+1,k-1} - F_{i-1,j+1,k-1}}{2h} \right) + \\ &\frac{\beta}{4} \left(\frac{F_{i+1,j-1,k+1} - F_{i-1,j-1,k+1} + F_{i+1,j-1,k-1} - F_{i-1,j-1,k-1}}{2h} \right) \end{aligned}$$

$$\begin{aligned} \frac{\partial F}{\partial z}(hi, hj, hk) &= (1 - \alpha - \beta) \frac{F_{i,j,k+1} - F_{i,j,k-1}}{2h} + \\ &\frac{\alpha}{4} \left(\frac{F_{i,j+1,k+1} - F_{i,j+1,k-1} + F_{i,j-1,k+1} - F_{i,j-1,k-1}}{2h} \right) + \\ &\frac{\alpha}{4} \left(\frac{F_{i+1,j,k+1} - F_{i-1,j,k+1} + F_{i+1,j,k-1} - F_{i-1,j,k-1}}{2h} \right) + \\ &\frac{\beta}{4} \left(\frac{F_{i+1,j+1,k+1} - F_{i-1,j+1,k+1} + F_{i+1,j-1,k+1} - F_{i-1,j-1,k+1}}{2h} \right) + \\ &\frac{\beta}{4} \left(\frac{F_{i+1,j+1,k-1} - F_{i-1,j+1,k-1} + F_{i+1,j-1,k-1} - F_{i-1,j-1,k-1}}{2h} \right) \end{aligned}$$

where α, β are given by:

$$\begin{aligned} \alpha &= 2\sqrt{2} - \frac{4}{3}\sqrt{3} \\ \beta &= 2 - 2\sqrt{2} + \frac{2}{3}\sqrt{3} \end{aligned}$$

3 Invariant computation of the principal directions and curvatures of a iso-intensity surface.

Principal directions and curvatures are a very important information in many 3D image applications, so we are interested in providing good estimations of such differential characteristics. First, we show how to compute the principal directions and curvatures from the first and second order derivatives. As far as we know, this technique is different from the ones proposed earlier in the literature of computer vision community. Let $\mathbf{x} = (x_1, x_2, x_3)$ be a point where the gradient $\nabla F(\mathbf{x})$ of the intensity function is different from 0, we consider the iso-intensity surface passing by \mathbf{x} . We use a Taylor development of function $F(\mathbf{x})$ but restricted to the tangent plane to the iso-intensity surface passing by \mathbf{x} . We notice that if we denote by \mathbf{e} the vector $\frac{\nabla F(\mathbf{x})}{\|\nabla F(\mathbf{x})\|}$, then for any 3D direction \mathbf{h} , the projection $P\mathbf{h}$ of \mathbf{h} in the tangent plane is given by:

$$P\mathbf{h} = (Id - \mathbf{e} \otimes \mathbf{e})\mathbf{h}$$

where \otimes means the tensor product. So in order to study the evolution of function F restricted to the tangent plane we consider the Taylor development:

$$\begin{aligned} F(\mathbf{x} + P\mathbf{h}) &= F(\mathbf{x}) + (P\mathbf{h})^T \nabla F(\mathbf{x}) + (P\mathbf{h})^T \nabla^2 F(\mathbf{x}) P\mathbf{h} = \\ &= F(\mathbf{x}) + \mathbf{h}^T P^T \nabla^2 F(\mathbf{x}) P\mathbf{h} \end{aligned}$$

since $(P\mathbf{h})^T \nabla F(\mathbf{x}) = 0$. Now, if we consider the matrix $A = P^T \nabla^2 F(\mathbf{x}) P$, it is easy to show that A has the eigenvalue 0 which corresponds to eigenvector given by the gradient direction \mathbf{e} and that the other eigenvectors of A correspond to the principal directions. On the other hand, if we consider that λ_1 and λ_2 are the other eigenvalues of A , then the principal curvatures k_i are given by

$$k_i = \frac{\lambda_i}{\|\nabla F(\mathbf{x})\|} \quad i = 1, 2$$

So, as the reader can realize, this procedure provides a very simple way to compute the principal curvatures and directions of the iso-intensity surface.

We notice that, from a numerical point of view, the estimations of the principal directions and curvatures depend just on the way we discretize the gradient and the Hessian matrix. Since the way we discretize the gradient was fitted in the previous section, we focus our attention on the way we can discretize the Hessian in order to have a good estimation of the principal directions and curvatures. As in the previous section, we use again the 'ideal' edge given by the family of functions $F^e(\mathbf{x})$. In this case, we impose that principal curvatures k_1 and k_2 be equal to 0, independently of the orientation of the plane given by \mathbf{e} . Again, as in the previous section, if we impose that $k_1 = k_2 = 0$ for any $e_i \in \{-1, 0, 1\}$ then the second derivatives of F have to be computed in the following way:

$$\begin{aligned}
\frac{\partial^2 F}{\partial x^2}(hi, hj, hk) &= (1 - \alpha - \beta) \frac{F_{i+1,j,k} + F_{i-1,j,k} - 2F_{i,j,k}}{h^2} + \\
&\frac{\alpha}{4} \left(\frac{F_{i+1,j+1,k} + F_{i-1,j+1,k} - 2F_{i,j+1,k} + F_{i+1,j-1,k}}{h^2} \right) + \\
&\frac{\alpha}{4} \left(\frac{F_{i-1,j-1,k} - 2F_{i,j-1,k} + F_{i-1,j,k-1} - 2F_{i,j,k-1}}{h^2} \right) + \\
&\frac{\alpha}{4} \left(\frac{F_{i+1,j,k+1} + F_{i-1,j,k+1} - 2F_{i,j,k+1} + F_{i+1,j,k-1}}{h^2} \right) + \\
&\frac{\beta}{4} \left(\frac{F_{i+1,j+1,k+1} + F_{i-1,j+1,k+1} - 2F_{i,j+1,k+1} + F_{i+1,j-1,k+1}}{h^2} \right) + \\
&\frac{\beta}{4} \left(\frac{F_{i-1,j-1,k+1} - 2F_{i,j-1,k+1} + F_{i-1,j-1,k-1} - 2F_{i,j-1,k-1}}{h^2} \right) + \\
&\frac{\beta}{4} \left(\frac{F_{i+1,j+1,k-1} + F_{i-1,j+1,k-1} - 2F_{i,j+1,k-1} + F_{i+1,j-1,k-1}}{h^2} \right)
\end{aligned}$$

$$\begin{aligned}
\frac{\partial^2 F}{\partial y^2}(hi, hj, hk) &= (1 - \alpha - \beta) \frac{F_{i,j+1,k} + F_{i,j-1,k} - 2F_{i,j,k}}{h^2} + \\
&\frac{\alpha}{4} \left(\frac{F_{i+1,j+1,k} + F_{i-1,j-1,k} - 2F_{i+1,j,k} + F_{i-1,j+1,k}}{h^2} \right) + \\
&\frac{\alpha}{4} \left(\frac{F_{i-1,j-1,k} - 2F_{i-1,j,k} + F_{i,j-1,k-1} - 2F_{i,j,k-1}}{h^2} \right) + \\
&\frac{\alpha}{4} \left(\frac{F_{i,j+1,k+1} + F_{i,j-1,k+1} - 2F_{i,j,k+1} + F_{i,j+1,k-1}}{h^2} \right) + \\
&\frac{\beta}{4} \left(\frac{F_{i+1,j+1,k+1} + F_{i+1,j-1,k+1} - 2F_{i+1,j,k+1} + F_{i-1,j+1,k-1}}{h^2} \right) + \\
&\frac{\beta}{4} \left(\frac{F_{i-1,j-1,k-1} - 2F_{i-1,j,k-1} + F_{i+1,j-1,k-1} - 2F_{i+1,j,k-1}}{h^2} \right) + \\
&\frac{\beta}{4} \left(\frac{F_{i-1,j+1,k+1} + F_{i-1,j-1,k+1} - 2F_{i-1,j,k+1} + F_{i+1,j+1,k-1}}{h^2} \right)
\end{aligned}$$

$$\begin{aligned}
\frac{\partial^2 F}{\partial z^2}(hi, hj, hk) &= (1 - \alpha - \beta) \frac{F_{i,j,k+1} + F_{i,j,k-1} - 2F_{i,j,k}}{h^2} + \\
&\frac{\alpha}{4} \left(\frac{F_{i+1,j,k+1} + F_{i+1,j,k-1} - 2F_{i+1,j,k} + F_{i-1,j,k+1}}{h^2} \right) + \\
&\frac{\alpha}{4} \left(\frac{F_{i-1,j,k-1} - 2F_{i-1,j,k} + F_{i,j-1,k-1} - 2F_{i,j-1,k}}{h^2} \right) + \\
&\frac{\alpha}{4} \left(\frac{F_{i,j+1,k+1} + F_{i,j+1,k-1} - 2F_{i,j+1,k} + F_{i,j-1,k+1}}{h^2} \right) + \\
&\frac{\beta}{4} \left(\frac{F_{i+1,j+1,k+1} + F_{i+1,j+1,k-1} - 2F_{i+1,j+1,k} + F_{i-1,j-1,k+1}}{h^2} \right) + \\
&\frac{\beta}{4} \left(\frac{F_{i-1,j-1,k-1} - 2F_{i-1,j-1,k} + F_{i+1,j-1,k-1} - 2F_{i+1,j-1,k}}{h^2} \right) + \\
&\frac{\beta}{4} \left(\frac{F_{i-1,j+1,k+1} + F_{i-1,j+1,k-1} - 2F_{i-1,j+1,k} + F_{i+1,j-1,k+1}}{h^2} \right)
\end{aligned}$$

$$\begin{aligned}
\frac{\partial^2 F}{\partial x \partial y}(hi, hj, hk) &= \\
&(1 - \gamma) \frac{F_{i+1,j+1,k} + F_{i-1,j-1,k} - F_{i+1,j-1,k} - F_{i-1,j+1,k}}{4h^2} + \\
&\frac{\gamma}{2} \left(\frac{F_{i+1,j+1,k+1} + F_{i-1,j-1,k+1} - F_{i+1,j-1,k+1} - F_{i-1,j+1,k+1}}{4h^2} \right) \\
&\frac{\gamma}{2} \left(\frac{F_{i+1,j+1,k-1} + F_{i-1,j-1,k-1} - F_{i+1,j-1,k-1} - F_{i-1,j+1,k-1}}{4h^2} \right)
\end{aligned}$$

$$\begin{aligned} \frac{\partial^2 F}{\partial x \partial z}(hi, hj, hk) = & \\ (1 - \gamma) \frac{F_{i+1,j,k+1} + F_{i-1,j,k-1} - F_{i+1,j,k-1} - F_{i-1,j,k+1}}{4h^2} + & \\ \frac{\gamma}{2} \left(\frac{F_{i+1,j+1,k+1} + F_{i-1,j+1,k-1} - F_{i+1,j+1,k-1} - F_{i-1,j+1,k+1}}{4h^2} \right) + & \\ \frac{\gamma}{2} \left(\frac{F_{i+1,j-1,k+1} + F_{i-1,j-1,k-1} - F_{i+1,j-1,k-1} - F_{i-1,j-1,k+1}}{4h^2} \right) & \end{aligned}$$

$$\begin{aligned} \frac{\partial^2 F}{\partial y \partial z}(hi, hj, hk) = & \\ (1 - \gamma) \frac{F_{i,j+1,k+1} + F_{i,j-1,k-1} - F_{i,j+1,k-1} - F_{i,j-1,k+1}}{4h^2} + & \\ \frac{\gamma}{2} \left(\frac{F_{i+1,j+1,k+1} + F_{i+1,j-1,k-1} - F_{i+1,j+1,k-1} - F_{i+1,j-1,k+1}}{4h^2} \right) + & \\ \frac{\gamma}{2} \left(\frac{F_{i-1,j+1,k+1} + F_{i-1,j-1,k-1} - F_{i-1,j+1,k-1} - F_{i-1,j-1,k+1}}{4h^2} \right) & \end{aligned}$$

where α, β and γ , satisfy the relations:

$$\begin{aligned} \beta &= \frac{1}{2} - \frac{1}{2}\alpha \\ \gamma &= 5\alpha - 2 \end{aligned}$$

in order to fit the value of α , we impose that all the coefficients which appear in the derivative estimations, that is $\alpha, \beta(\alpha), \gamma, (1 - \alpha - \beta(\alpha)), (1 - \gamma(\alpha))$, be in $[0, 1]$, with this assumption we ensure that the balance of the above coefficients represents an average of derivative estimations. In figure (1) we illustrate the shape of such functions.

We notice that the value $\alpha = 0.5$ (which corresponds to the intersection point in the figure) minimizes all the functions simultaneously. With this value of $\alpha = 0.5$ we obtain that $\beta = 0.25$ and $\gamma = 0.5$.

4 Numerical Experiences

We compare our method with 2 classical schemes to compute the derivatives of an image. As it is usually done (see for instance [3]), we introduce a convolution with a Gaussian function in the derivative estimations. In the first method, the derivatives are computed by convolving the image with the derivatives of the Gaussian, that is :

$$\frac{\partial^\alpha F}{\partial x_1^{\alpha_1} \dots \partial x_N^{\alpha_N}} \cong \frac{\partial^\alpha G_\sigma}{\partial x_1^{\alpha_1} \dots \partial x_N^{\alpha_N}} * F \quad (1)$$

where $G_\sigma(\cdot)$ is the Gaussian function with standard deviation σ . In order to compute these derivatives we take advantage of the separability of the gaussian kernel and we use

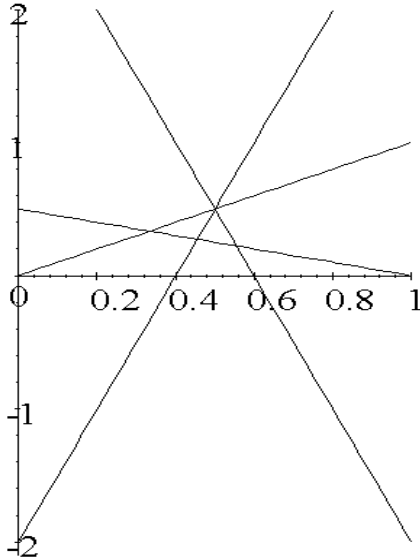


Figure 1: Shape of functions α , $\beta(\alpha)$, $\gamma(\alpha)$, $(1 - \alpha - \beta(\alpha))$, $(1 - \gamma(\alpha))$

recursive schemes as the ones proposed in [1]. In the second method, we compute the derivatives of the function $F(\cdot)$ using the usual central finite difference schemes, that is $\partial F / \partial x \cong (F(x+h, y, z) - F(x-h, y, z)) / 2$, and so on. However, in order to compare this estimation with the previous one, we convolve the image $F(\cdot)$ with a Gaussian function before computing the derivatives, that is, we compute

$$\frac{\partial^\alpha F}{\partial x_1^{\alpha_1} \dots \partial x_N^{\alpha_N}} \cong \frac{\partial^\alpha (G_\sigma * F)}{\partial x_1^{\alpha_1} \dots \partial x_N^{\alpha_N}} \quad (2)$$

In order to compute our derivative estimations, we also convolve the image $F(\cdot)$ with the gaussian function $G_\sigma(\cdot)$ previously. The difference between (2) and our method is that we use the invariant estimation of the derivatives instead of the usual central difference estimations.

In the first numerical experience, we present comparison results on a synthetic sphere of radius 50 voxels. This image is generated by taking into account a Partial Volume Effect: the value of the intensity of the voxel is proportional to the volume of the sphere inside the voxel. Theoretically, on the voxels that belong to the frontier of the sphere, we expect to find out that the norm of the gradient as well as the principal curvatures be constant. We fit the standard deviation σ of the Gaussian function equal to 1 in all the numerical experiments.

In table 1, we present the minimum, the maximum, the mean, the standard deviation and the ratio between the standard deviation and the mean of the norm of the gradient on the sphere using the different methods. We notice that this ratio determines the accuracy

	min	max	mean	st.dev.	sd/mean
Meth. (2)	31.30	36.44	34.22	1.18	0.035
Meth. (1)	34.68	38.33	37.19	0.89	0.024
Paper	30.30	32.64	31.54	0.59	0.019

Table 1: Norm of the gradient estimations on the sphere

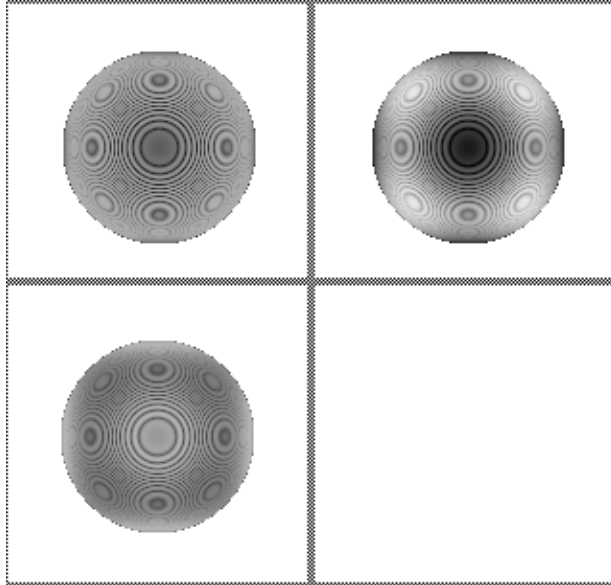


Figure 2: Visualization using a MIP projection of the norm of the gradient in the sphere. From left to right and from top to bottom we present the results with method (1), method (2) and the method proposed in this paper.

of the estimation (the lower the ratio, the better the estimation). It can be seen that our proposed method gives the most uniform estimation of the norm of the gradient. In figure 2, we present a Maximum Intensity Projection (MIP) of the value of the norm of the gradient on the sphere. The fluctuations of the grey-level in figure 2 determine the numerical error of the methods.

In tables 2 and 3 we present the results of the estimations of the principal curvatures on the sphere. We also obtain a lower ratio than the other methods. Moreover, our method is the only one that does not produce negative curvatures.

In figure 3 we present a MIP projection of the principal curvatures on the sphere. The fluctuations of the grey-level determine the numerical error of the methods. We can visually appreciate that the image produced by our method is more uniform.

In the second experiment we present some results on a real image given by an angiography (see figure 4). In figure 5, we present the estimation of the norm of the gradient. Figures 6 and 7 show the estimation of the minimal and maximal curvature. Whereas the

	min	max	mean	st.dev.	sd/mean
Meth. (2)	-0.021	0.033	0.013	0.015	1.142
Meth. (1)	-0.011	0.026	0.017	0.008	0.450
Paper	0.005	0.0247	0.019	0.004	0.182

Table 2: Minimal curvature estimations on the sphere

	min	max	mean	st.dev.	sd/mean
Meth. (2)	-0.023	0.064	0.013	0.015	0.477
Meth. (1)	0.018	0.052	0.024	0.007	0.306
Paper	0.018	0.036	0.023	0.003	0.134

Table 3: Maximal curvature estimations on the sphere

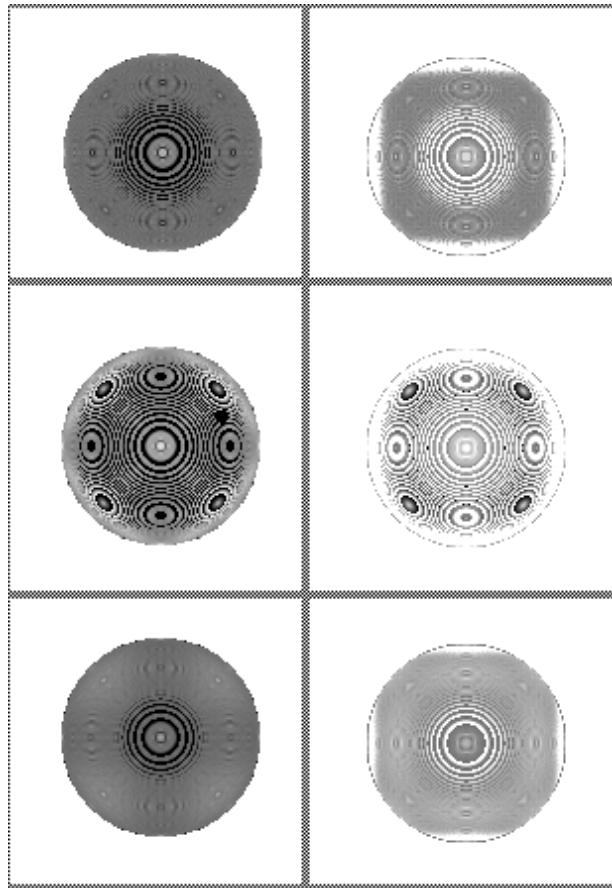


Figure 3: Visualization using a MIP projection of the principal curvatures on the sphere. Left column shows the minimal curvature. Right column shows the maximal curvature. From top to bottom we present the results of method (1) method (2) and the proposed method.



Figure 4: Isointensity Surface of the angiography



Figure 5: Norm of the Gradient estimation on the angiography

minimal curvature is almost constant, the maximal curvature is higher for thinner vessels.

In order to perform some numerical comparisons between the different methods, we select a sub-volume of the angiography that corresponds to one vessel with approximately constant cross-section. Figure 8 shows an isosurface of this sub-image. In this experiment, we expect to find small variations of the norm of gradient and of the maximal curvature on the contour of the vessel.

Table 4 and 5 present the results of the estimations of the norm of the gradient and the maximal curvature on the voxels of the contour. Our method still gives better results for the ratio.



Figure 6: Minimal curvature estimation on the angiography



Figure 7: Maximal curvature estimation on the angiography

	min	max	mean	st.dev.	sd/mean
Meth. (2)	360.5	953.8	645.2	129.5	0.201
Meth. (1)	360.8	1113	668.2	147.4	0.221
Paper	360.9	900	617.0	117.7	0.191

Table 4: Norm of the gradient estimations on the vessel in fig. 9

	min	max	mean	st.dev.	sd/mean
Meth. (2)	-0.221	0.706	0.258	0.116	0.449
Meth. (1)	-0.261	0.675	0.251	0.121	0.484
Paper	-0.199	0.700	0.265	0.113	0.428

Table 5: Maximal curvature estimations on the vessel in fig. 11



Figure 8: Isointensity surface on the vessel.



Figure 9: Norm of the gradient estimation on the vessel.

Finally in figure 9 we present the estimation of the norm of the gradient on the vessel. Figures 10 and 11 present the estimation of the minimal and maximal curvature. As observed, the minimal curvature varies with the small variations of the radius of the vessel. The maximal curvature is more homogeneous, but gives white lines due to the elliptical shape of the cross-section.

5 Conclusions

In this paper we have proposed a new technique to compute the first and second derivatives of a 3D image based on the rotation invariance of some important differential character-

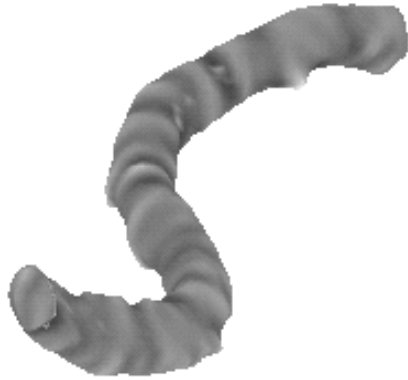


Figure 10: Minimal curvature estimation on the vessel.



Figure 11: Maximal curvature estimation on the vessel

istics like the magnitude of the gradient and the principal curvatures of an iso-intensity surface. Preserving such a rotation invariance in the discrete implementation is very important in order to discriminate points in the image. The numerical results show that this new technique preserves the rotation invariance better than the usual estimations specially in the case of the principal curvatures.

References

- [1] R. Deriche, "Recursively implementing the Gaussian and its derivatives" in *Proc. Second International Conference on Image Processing*, pp. 263-267, Singapore, 1992.
- [2] K. Krissian, G. Malandain, N. Ayache, "Directional Anisotropic Diffusion Applied to Segmentation of Vessels in 3D Images" *Scale-Space Theory in Computer Vision*, Lecture Notes in Computer Science V. 1252 pp. 345-348, 1997.
- [3] T. Lindeberg, "Scale-Space theory in Computer Vision" *Kluwer Academic Publishers*, 1994.
- [4] L. Lorigo, O. Faugeras, W.E.L. Grimson, R. Keriven, R. Kikinis, and C-F Westin, "Co-Dimension 2 Geodesic Active Contours for MRA Segmentation" *International Conference on Information Processing in Medical Imaging (IPMI)*, Lecture Notes in Computer Science V. 1613 pp. 126-139, 1999.
- [5] O. Monga, N. Ayache and P. Sander, "From Voxel to curvature," *Computer Vision and Pattern Recognition*, pp. 644-649, IEEE, Washington, DC, 1991.
- [6] O. Monga, S. Benayoun and O. Faugeras, "Using partial derivatives of 3D images to extract typical surface features," in *Proceedings CVPR'92, Urbana Champaign, IEEE, July 1992*. , Also INRIA Research Report 1599.
- [7] J-P. Thirion and A. Gourdon, "Computing the differential characteristic of iso-intensity surfaces," *Computer Vision and Image Understanding*, Vol. 61, No. 2 pp. 190-202, 1995.